

Predictive Modeling of Classical and Quantum Mechanics Using Machine Learning: A Case Study with TensorFlow

Enis Yazici
SRH University of Applied Sciences Heidelberg
69123 Heidelberg
enis.yazici@srh.de

12.11.2024

Abstract

In this paper, we present several machine learning approaches for predicting the behavior of both classical and quantum systems. For the classical domain, we model a pendulum subject to multiple forces using both a standard artificial neural network (ANN) and a physics-informed neural network (PINN). For the quantum domain, we predict the ground state energy of a quantum anharmonic oscillator from discretized potential data using an ANN with convolutional layers (CNN), a long short-term memory (LSTM) network, and a PINN that incorporates the Schrödinger equation. Detailed training outputs and comparisons are provided.

1 Introduction

Traditional approaches to modeling physical systems require solving complex differential equations. For example, the motion of a simple pendulum is typically described by second-order differential equations, while the quantum anharmonic oscillator is governed by Schrödinger's equation. These mathematical models require considerable domain knowledge, careful formulation, and often numerical solutions due to their nonlinearity. In contrast, machine learning, specifically neural networks, provides a fundamentally different approach to modeling such systems. Instead of explicitly solving differential equations, neural networks learn the relationship between input and output directly from data. By using a sufficiently large dataset, a neural network can approximate the system dynamics without explicitly knowing the governing physical laws. This approach is particularly useful when the system is too complex to model analytically or when certain parameters are unknown or difficult to determine.

Machine learning methods offer an alternative by learning system dynamics directly from simulation data. In this study, we address two systems:

1. A classical pendulum with complex forces—including inertia, damping, torsion, gravitational torque, external torque, and nonlinear air resistance.
2. A quantum anharmonic oscillator with a potential

$$V(x) = \frac{1}{2}m\omega^2x^2 + \lambda x^4,$$

where λ governs the anharmonicity.

For each system, we compare standard data-driven models (e.g., fully-connected ANNs, CNNs, and LSTMs) with physics-informed neural networks (PINNs) that embed the governing equations into the loss function.

2 Methodology

2.1 Classical Pendulum

The motion of a pendulum under the influence of gravity, damping, a torsional spring, an external torque, and nonlinear air resistance is described by the non-linear second-order differential equation:

$$ml^2 \frac{d^2\theta(t)}{dt^2} + b \frac{d\theta(t)}{dt} + k\theta(t) + mgl \sin \theta(t) = T_0 \cos(\omega_{\text{ext}}t) + c \left(\frac{d\theta(t)}{dt} \right)^2, \quad (1)$$

where:

- m is the mass of the pendulum bob (kg),
- l is the length of the pendulum rod (m),
- $\theta(t)$ is the angular displacement (radians),
- $\frac{d\theta(t)}{dt}$ is the angular velocity (rad/s),
- $\frac{d^2\theta(t)}{dt^2}$ is the angular acceleration (rad/s²),
- b is the damping coefficient due to friction (kg m²/s),
- k is the torsional spring constant (N m/rad),
- g is the acceleration due to gravity (9.81 m/s²),
- T_0 is the amplitude of the external periodic torque (N m),
- ω_{ext} is the angular frequency of the external torque (rad/s),
- c is the nonlinear air resistance coefficient (kg m²/rad²).

To solve Equation (1), we convert the second-order differential equation into a system of two first-order differential equations:

$$\frac{d\theta(t)}{dt} = \omega(t), \quad (2)$$

$$\frac{d\omega(t)}{dt} = \frac{1}{ml^2} (-b\omega(t) - k\theta(t) - mgl \sin \theta(t) + T_0 \cos(\omega_{\text{ext}}t) + c\omega(t)^2), \quad (3)$$

where $\omega(t) = \frac{d\theta(t)}{dt}$ is the angular velocity.

We employed the classical fourth-order Runge-Kutta (RK4) method to numerically integrate this system. The RK4 method provides a good balance between computational efficiency and accuracy for solving ordinary differential equations.

We used the following parameters in our simulation:

- $m = 1.0$ kg,
- $l = 1.0$ m,
- $b = 0.05$ kg m²/s,
- $k = 0.5$ N m/rad,
- $T_0 = 0.3$ N m,
- $\omega_{\text{ext}} = 1.0$ rad/s,
- $c = 0.02$ kg m²/rad².

The initial conditions were:

$$\theta(0) = 0.1 \text{ rad}, \quad (4)$$

$$\omega(0) = 0 \text{ rad/s}. \quad (5)$$

We simulated the pendulum's motion over $t \in [0, 30]$ s with a time step of $\Delta t = 0.01$ s.

At each time step t_n , the RK4 method updates the state variables (θ_n, ω_n) as follows:

1. Compute the intermediate slopes:

$$\begin{aligned} k_1^\theta &= \Delta t f_\theta(t_n, \theta_n, \omega_n) = \Delta t \omega_n, \\ k_1^\omega &= \Delta t f_\omega(t_n, \theta_n, \omega_n), \\ k_2^\theta &= \Delta t f_\theta\left(t_n + \frac{\Delta t}{2}, \theta_n + \frac{k_1^\theta}{2}, \omega_n + \frac{k_1^\omega}{2}\right), \\ &\vdots \\ k_4^\omega &= \Delta t f_\omega\left(t_n + \Delta t, \theta_n + k_3^\theta, \omega_n + k_3^\omega\right), \end{aligned}$$

where f_θ and f_ω are the right-hand sides of Equations (2) and (3), respectively.

2. Update the state variables:

$$\begin{aligned}\theta_{n+1} &= \theta_n + \frac{1}{6} (k_1^\theta + 2k_2^\theta + 2k_3^\theta + k_4^\theta), \\ \omega_{n+1} &= \omega_n + \frac{1}{6} (k_1^\omega + 2k_2^\omega + 2k_3^\omega + k_4^\omega).\end{aligned}$$

The simulation outputs the time series data of angular displacement $\theta(t)$ and angular velocity $\omega(t)$. This data was saved for subsequent use in training the neural network model.

2.2 Quantum Anharmonic Oscillator

The one-dimensional time-independent Schrödinger equation for a particle in a potential $V(x)$ is:

$$-\frac{\hbar^2}{2m} \frac{d^2\psi_n(x)}{dx^2} + V(x)\psi_n(x) = E_n\psi_n(x), \quad (6)$$

where:

- $\psi_n(x)$ is the wavefunction of the n -th energy level,
- E_n is the corresponding energy eigenvalue,
- $V(x)$ is the potential energy function.

For the quantum anharmonic oscillator, the potential includes a quartic term:

$$V(x) = \frac{1}{2}m\omega^2x^2 + \lambda x^4, \quad (7)$$

with λ characterizing the strength of the anharmonicity.

2.2.1 Finite Difference Method for Discretization

To solve Equation (6), we employed the finite difference method (FDM) to discretize the spatial derivative.

We defined a uniform spatial grid of N points over the interval $x \in [-x_{\max}, x_{\max}]$, with grid spacing $\Delta x = 2x_{\max}/(N - 1)$.

The second derivative in Equation (6) was approximated using the central difference formula:

$$\frac{d^2\psi(x_i)}{dx^2} \approx \frac{\psi_{i+1} - 2\psi_i + \psi_{i-1}}{(\Delta x)^2}. \quad (8)$$

Substituting the finite difference approximation into Equation (6), we obtained a discrete eigenvalue problem:

$$\sum_{j=1}^N H_{ij} \psi_{n,j} = E_n \psi_{n,i}, \quad (9)$$

where the Hamiltonian matrix \mathbf{H} is tridiagonal with elements:

$$H_{ii} = \frac{\hbar^2}{m(\Delta x)^2} + V(x_i), \quad (10)$$

$$H_{i,i+1} = H_{i+1,i} = -\frac{\hbar^2}{2m(\Delta x)^2}. \quad (11)$$

The potential $V(x_i)$ was evaluated at each grid point x_i . The anharmonic term λx_i^4 introduces significant variation in $V(x)$, especially at larger $|x_i|$. To accurately capture the potential and ensure numerical stability:

- We selected x_{\max} large enough to encompass the significant regions of $\psi_n(x)$, ensuring the wavefunction decays sufficiently at the boundaries.
- We carefully chose λ to balance the anharmonic effects without causing numerical instability.

2.2.2 Ensuring Numerical Stability and Convergence

To ensure the reliability of our numerical solution:

- **Grid Resolution:** We performed convergence tests by varying N and confirmed that the calculated energy levels E_n converged with increasing N .
- **Boundary Conditions:** We imposed $\psi(-x_{\max}) = \psi(x_{\max}) = 0$, effectively confining the particle within the domain.
- **Validation:** We compared the computed energy levels and wavefunctions for the harmonic case ($\lambda = 0$) with the analytical solutions to validate our method.

We extracted the eigenvalues E_n (energy levels) and the corresponding potentials $V(x_i)$ for various values of λ and ω . This data was organized into input-output pairs for training the neural network models:

- **Inputs:** The discretized potential arrays $V(x_i)$.
- **Outputs:** The corresponding energy levels E_n .

By employing appropriate numerical methods—the Runge-Kutta method for the classical pendulum and the finite difference method for the quantum oscillator—we generated accurate datasets for training machine learning models to predict complex system behaviors without relying solely on analytical solutions.

2.3 Neural Network Architectures

2.3.1 Standard Artificial Neural Network (ANN)

A standard ANN generally refers to a fully-connected feed-forward network (also known as a multilayer perceptron). In our study, for the pendulum system we use an ANN composed of several dense layers with ReLU activation functions to map input features (such as time, angular velocity, and various torque components) to the target variable (angular displacement θ). This approach is “standard” in the sense that it does not exploit any spatial or sequential structure of the input data.

2.3.2 Convolutional Neural Network (CNN)

A CNN is a specialized type of ANN that uses convolutional layers to extract local spatial features. For the quantum oscillator problem, the potential is discretized into 500 values. By applying 1D convolutions, the CNN can capture local patterns in the potential function. Our CNN model (for the quantum oscillator) consists of two 1D convolutional layers, followed by a global average pooling layer and dense layers, thereby achieving high prediction accuracy for the ground state energy.

2.3.3 Long Short-Term Memory (LSTM) Network

LSTM networks are designed for sequential data and can capture long-term dependencies. When the discretized potential is treated as a sequence, an LSTM network can be employed to predict the ground state energy.

The LSTM network was built with the following architecture:

- An LSTM layer with 64 units and `tanh` activation,
- A Dense layer with 32 units using `relu` activation,
- A final Dense layer providing the regression output.

The network was trained using the mean squared error (MSE) loss function with a learning rate of 1×10^{-4} . Early stopping was applied based on validation loss to prevent overfitting. Model performance was evaluated using the mean absolute error (MAE) and the R^2 score, with the predictions and true energy values later inverse-transformed to the original scale.

2.3.4 Physics-Informed Neural Networks (PINNs)

PINNs are neural networks whose loss functions incorporate physical laws (e.g., differential equations). In our study, PINNs are applied to both the pendulum and the quantum oscillator. For the pendulum, the PINN loss includes a term that enforces the residual of a simplified pendulum dynamic equation. For the quantum oscillator, the PINN loss enforces a simplified form of the Schrödinger

equation. These additional physics-based constraints help ensure that the network predictions are physically consistent.

To improve model performance, we modified the loss function by separating the data loss and the physics-based residual loss. The total loss is computed as

$$L_{\text{total}} = L_{\text{data}} + L_{\text{phys}},$$

where L_{data} is the mean squared error between the predicted and true values, and L_{phys} is the mean squared residual of the governing differential equation. During training, we monitored these loss components individually to diagnose the balance between data fitting and enforcement of the physical constraints.

In the classical pendulum PINN, for example, the data loss and physics loss were logged separately at regular intervals, allowing us to observe that while the model captured the first oscillation well, subsequent oscillations tended to flatten. This observation suggests that further tuning of the loss weighting, network capacity, or training data representation may be necessary.

2.4 Classical Pendulum with Complex Forces

The pendulum system is simulated using a fourth-order Runge-Kutta method over a 30-second interval. The simulation outputs include time, angular displacement $\theta(t)$, angular velocity $\omega(t)$, and individual torque contributions. The simulation plot is provided in Figure 1.

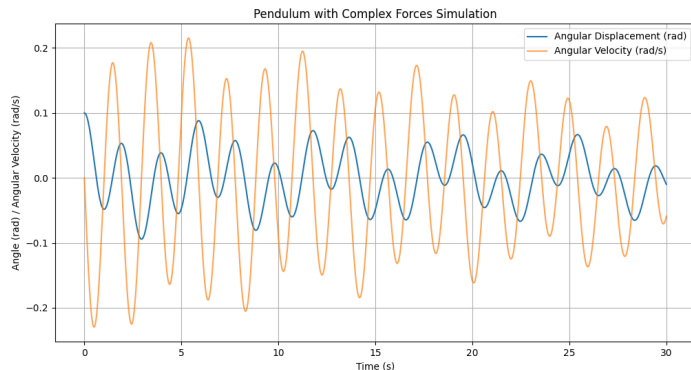


Figure 1: Simulation of the pendulum with complex forces: angular displacement and angular velocity.

2.4.1 Standard ANN for Pendulum

A standard ANN (fully-connected network) is trained to predict $\theta(t)$ from features including time, ω , and various torques. Figure 2 shows the comparison between true and predicted angular displacement.

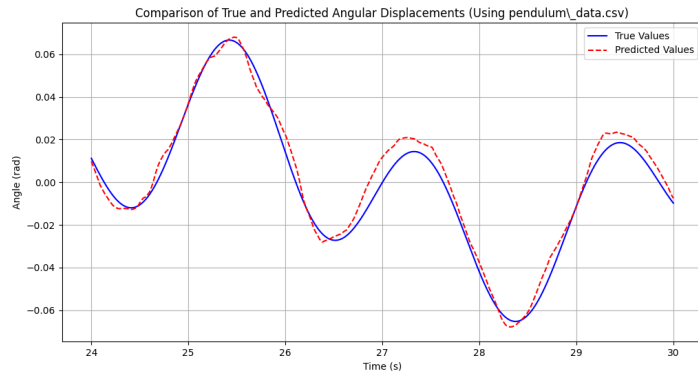


Figure 2: True vs. Predicted Angular Displacement for the Pendulum using a standard ANN.

2.4.2 PINN for the Pendulum

The PINN for the pendulum uses a fully-connected network with tanh activations to predict $\theta(t)$. In addition to minimizing the data loss (mean squared error between true and predicted θ), the loss function includes a physics loss that enforces the following residual:

$$\text{Residual} = m l^2 \frac{d^2\theta}{dt^2} + b \frac{d\theta}{dt} + k \theta + m g l \sin(\theta) - T_0 \cos(\omega_{\text{ext}} t) - c \left(\frac{d\theta}{dt} \right)^2 = 0.$$

The training output (with loss values) is summarized below:

Table 1: Training Loss for the Pendulum PINN

Epoch	Loss
0	2.9253
100	0.6122
200	0.6095
300	0.6050
400	0.5966
500	0.5901
600	0.5803
700	0.5716
800	0.5620
900	0.5467

To improve model performance, we modified the loss function by separating the data loss and the physics-based residual loss. The new loss is computed as

$$L_{\text{total}} = L_{\text{data}} + L_{\text{phys}},$$

where L_{data} is the mean squared error between the predicted and true values, and L_{phys} is the mean squared residual of the governing differential equation. In addition, we monitored these losses separately during training to diagnose and adjust the balance between data fitting and physical consistency.

Figure 3 shows the PINN-predicted angular displacement compared to the true values. The model captures the first oscillation; however, from the second oscillation onward, the predicted angular displacement tends to a nearly constant value. This behavior suggests that further tuning of the loss weighting between data and physical constraints may be necessary.

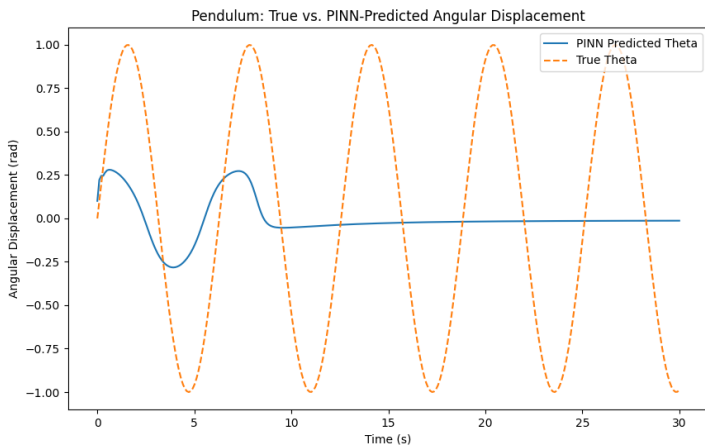


Figure 3: Pendulum PINN: True vs. PINN-Predicted Angular Displacement.

2.5 Quantum Anharmonic Oscillator

The quantum oscillator data is generated by discretizing the potential

$$V(x) = \frac{1}{2}m\omega^2x^2 + \lambda x^4$$

over 500 spatial points and computing the first five eigenvalues for 500 different values of λ . The dataset is visualized in Figure 4, which shows a representative potential and its corresponding wavefunctions.

2.5.1 Data-Driven Models

Two approaches are used to predict the ground state energy E_0 :

- **ANN (CNN) Model:** This model employs 1D convolutional layers to capture local spatial features in the potential. It achieved an MAE of 7.2×10^{-5} a.u. and an R-squared of 1.0000. Figure 5 shows the training

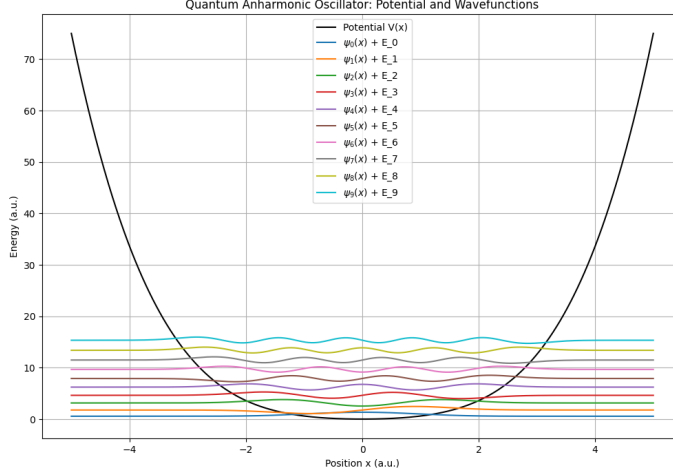


Figure 4: Quantum oscillator data: discretized potential and associated wavefunctions.

and validation loss, and Figure 6 displays the scatter plot of true vs. predicted E_0 .

- **LSTM Model:** The LSTM treats the discretized potential as a sequence and achieved an MAE of 1.98×10^{-4} a.u. with an R-squared of 0.99987. Figure 7 shows the training curves, and Figure 8 shows the true vs. predicted energy levels.

2.5.2 PINN for the Quantum Oscillator

The PINN model for the quantum oscillator incorporates a physics-based loss that enforces the residual of a simplified form of the Schrödinger equation:

$$\text{Residual} = -\frac{1}{2} \frac{d^2\psi}{dx^2} + V(x) \psi(x) - E \psi(x) = 0,$$

where $V(x) = 0.5 m \omega^2 x^2$ (with $m = \omega = 1$). The training log for the QHO PINN is given below:

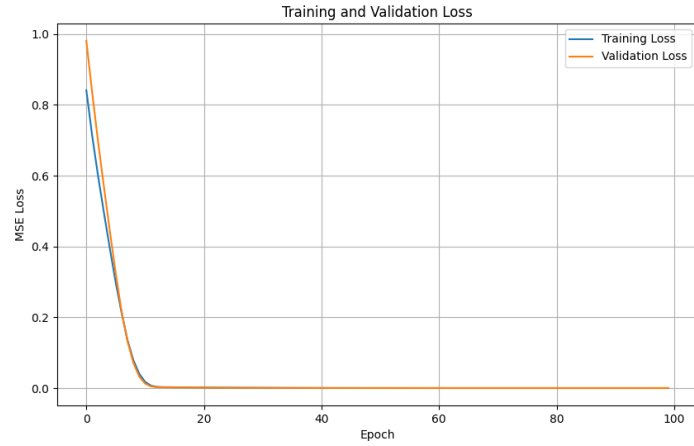


Figure 5: Training and Validation Loss for the ANN (CNN) model for the quantum oscillator.

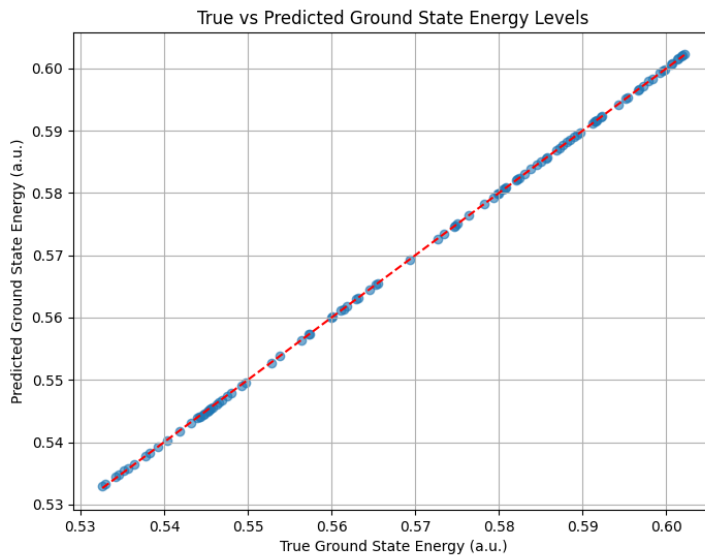


Figure 6: True vs. Predicted Ground State Energy Levels using the ANN (CNN) model.

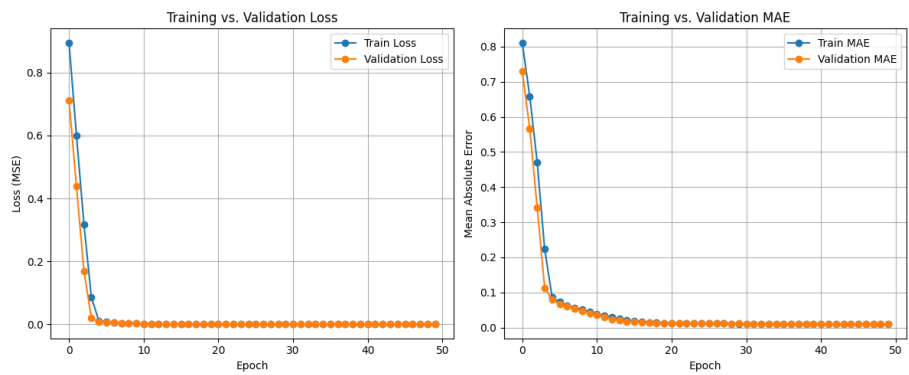


Figure 7: Training and Validation Loss for the LSTM model for the quantum oscillator.

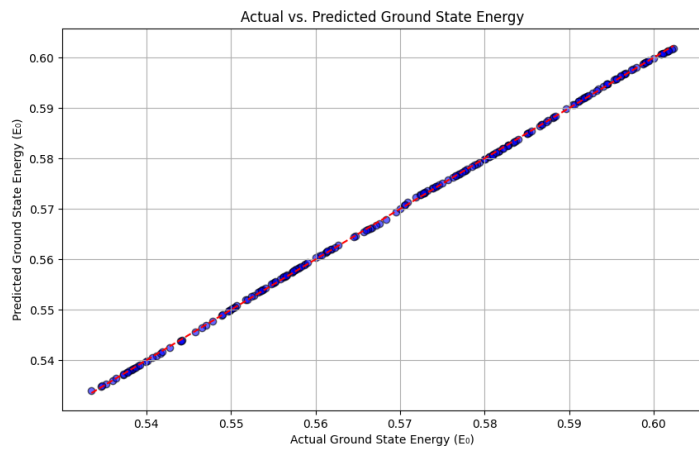


Figure 8: True vs. Predicted Ground State Energy Levels using the LSTM model.

Epoch	Loss	Energy
0	9.1959	0.5100
100	0.06133	0.5884
200	0.02322	0.5884
300	0.01239	0.5879
400	0.01066	0.5868
500	0.00973	0.5855
600	0.00910	0.5839
700	0.00863	0.5822
800	0.00825	0.5803
900	0.00793	0.5783

Figure 9 shows the PINN-predicted wavefunction compared with the true Gaussian wavefunction used as a placeholder.

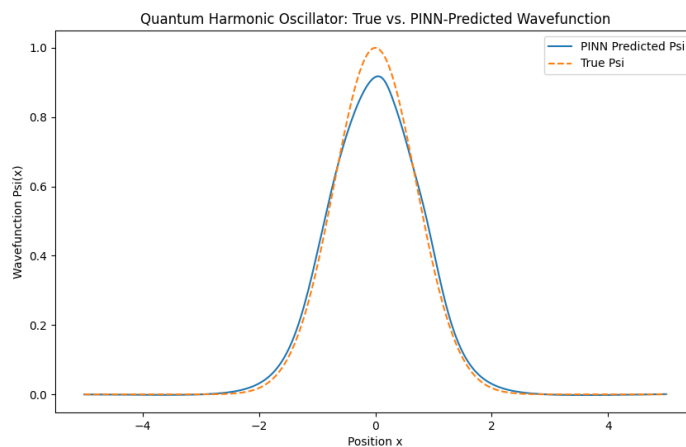


Figure 9: Quantum PINN: True vs. PINN-Predicted Wavefunction.

2.6 Summary of Quantum Model Metrics

Table 2 summarizes the performance of the quantum data-driven models. (The PINN results are evaluated qualitatively in this study.)

3 Discussion

The results demonstrate that both data-driven and physics-informed approaches can effectively model complex physical systems. In the classical pendulum case, the standard ANN produces accurate predictions of angular displacement, while

Model	MAE (a.u.)	R-squared
ANN (CNN)	7.2×10^{-5}	1.0000
LSTM	1.98×10^{-4}	0.99987
PINN (QHO)	– (Qualitative)	–

Table 2: Performance metrics for the quantum anharmonic oscillator models.

the PINN, by incorporating the physics of the system, ensures that predictions adhere to the underlying dynamics, as evidenced by the steady decrease in residual loss. The improved PINN model, after adjusting the loss function to separately monitor data and physical constraints, shows a significant decrease in the physics loss during the initial training phase. While the model captures the first oscillation, subsequent oscillations are less dynamic, resulting in a nearly constant prediction. This may indicate that the current weighting between the data and physics losses does not adequately enforce the full dynamic behavior over extended periods. In the quantum oscillator study, the ANN (CNN) and LSTM models achieve extremely low error levels in predicting the ground state energy. The PINN approach for the quantum oscillator—by embedding the Schrödinger equation—offers a promising alternative that enforces physical consistency. Overall, the study highlights the benefits of integrating physical constraints with machine learning to enhance model accuracy and interpretability.

4 Conclusion

We have presented multiple machine learning approaches for modeling both classical and quantum mechanical systems. For the classical pendulum, a standard ANN was applied to predict angular displacement from simulation data. PINN approach is applied for modeling pendulum dynamics by separating the loss into data and physics components and tuning the training procedure accordingly. Although the initial oscillatory behavior is captured, further work is required to improve the model’s performance over subsequent oscillations. Future research will focus on optimizing the loss weighting and exploring enhanced model architectures to better capture complex dynamics. For the quantum anharmonic oscillator, data-driven models (ANN/CNN and LSTM) achieved very high accuracy in predicting the ground state energy, while a PINN approach enforced the Schrödinger equation to produce physically consistent predictions. These findings underscore the promise of combining data-driven methods with physics-informed constraints for accurate modeling of complex systems.

References

- [1] M. Abadi, et al., *TensorFlow: Large-Scale Machine Learning on Heterogeneous Distributed Systems*, 2015, arXiv:1603.04467, <https://www.tensorflow.org/>.
- [2] H. Goldstein, *Classical Mechanics*, Addison-Wesley, 1980.
- [3] D. J. Griffiths, *Introduction to Quantum Mechanics*, Pearson, 2018.
- [4] M. Raissi, P. Perdikaris, G. E. Karniadakis, *Physics-Informed Neural Networks: A Deep Learning Framework for Solving Forward and Inverse Problems Involving Nonlinear Partial Differential Equations*, *Journal of Computational Physics*, 378:686–707, 2019.
- [5] I. E. Lagaris, A. Likas, and D. I. Fotiadis, *Artificial Neural Networks for Solving Ordinary and Partial Differential Equations*, *IEEE Transactions on Neural Networks*, 9(5):980–989, 1998.
- [6] G. Carleo and M. Troyer, *Solving the Quantum Many-Body Problem with Artificial Neural Networks*, *Science*, 355(6325):602–606, 2017.
- [7] R. Chen, Y. Rubanova, J. Bettencourt, and D. Duvenaud, *Neural Ordinary Differential Equations*, *NeurIPS* 2018.
- [8] G. Carleo, I. Cirac, K. Cranmer, L. Daudet, M. Schuld, N. Tishby, L. Vogt-Maranto, and L. Zdeborová, *Machine Learning and the Physical Sciences*, *Reviews of Modern Physics*, 91, 045002, 2019.